Engineering Geology 123 (2011) 60–71

Contents lists available at ScienceDirect

Engineering Geology

journal homepage: www.elsevier.com/locate/enggeo

The formation and breaching of a short-lived landslide dam at Hsiaolin Village, Taiwan — Part II: Simulation of debris flow with landslide dam breach

Ming-Hsu Li [a,*], Rui-Tang Sung [a], Jia-Jyun Dong [b], Chyi-Tyi Lee [b], Chien-Chih Chen [c]

[a] Graduate Institute of Hydrological and Oceanic Sciences, National Central University, No. 300, Jhongda Rd., Jhongli, Taiwan
[b] Graduate Institute of Applied Geology, National Central University, No. 300, Jhongda Rd., Jhongli, Taiwan
[c] Graduate Institute of Geophysics & Department of Earth Sciences, National Central University, No. 300, Jhongda Rd., Jhongli, Taiwan

ARTICLE INFO

Available online 10 May 2011

Keywords:
Typhoon Morakot
Landslide dam
Debris flow
FLO-2D
BREACH

ABSTRACT

Typhoon Morakot (2009) caused serious damage in southern Taiwan due to intensive rainfall with long duration. The issue of greatest concern arising from the disasters brought about by this extreme event was the burying of the entire village of Hsiaolin by a massive debris flow and landslide. Based on seismological and near-surface magnetic data, this tragic scenario arose due to a combination of events, a massive landslide, the formation of a landslide dam, and the consequent debris flow when this dam was breached. The objective of this part of the study is to investigate the spatial and temporal characteristics of the debris flow induced by the landslide breach. The US National Weather Service BREACH model and the Federal Emergency Management Agency approved FLO-2D model are integrated to facilitate the investigation of this catastrophe. A series of simulations including a 2D rainfall-runoff simulation over the Cishan River basin, landslide dam breach routing, and 2D debris flow simulation around the Hsiaolin Village were conducted. Hydraulic calculations were performed to determine the equivalent top elevation of the landslide dam based on inflows computed from the 2D rainfall-runoff simulation in association with the Digital Terrain Model (DTM) and upstream constraint of the backwater inundation areas. The hydrograph of the upstream inflow which induced overtopping failure was provided by a 2D rainfall-runoff simulation using the FLO-2D model calibrated by comparison with the downstream discharge record. The longevity of the landslide dam was less than 1 h, and it took only about 8 minutes to completely breach. The peak discharge rate of this massive landslide dam breach was 70,649 m^3/s. The dam break hydrograph was then used for upstream inflow to drive the FLO-2D debris flow simulation. The average sediment concentration by volume was 0.362. The simulated deposited sediment depth showed a reasonable match to the differences of DTMs before and after the disaster.

1. Introduction

An annual average of 3.6 typhoons invaded Taiwan and its vicinity and were recognized as one of the most devastating natural hazards for this island (Li et al., 2005). According to the observed rainfall at the Mintzu station, the daily rainfall of 8 August 2009 reached 1114 mm/day which is the highest daily amount since the gauge station was established in 1977 (Table 1). Owing to the intensive and long duration rainfalls events, the 3-day rainfall accumulation before gauge failure on 9 August was more than 1689 mm, which is more than 60% of the annual rainfall amount. Like many other typhoons that caused lowlands flooding and breaking of bridges, Typhoon Morakot (2009) shockingly destroyed the entire mountainous Hsiaolin Village and buried more than 400 people alive (Lee et al., 2009).

As described in Part I of this study (Dong et al., in press), the Hsiaolin tragedy occurred due to the combination of a massive landslide and the consequent breaching of the landslide dam. Extreme and continuous rainfalls triggered the massive landslide that blocked the gorge of the Cishan River to form a landslide dam in the early morning of August 9. Unlike any manmade gravity or concrete dam with engineered barriers and filter materials, a landslide dam is formed by an unconsolidated heterogeneous mixture of earth/rock debris in a naturally unstable state. Of about 55 failures of landslide dams reviewed by Costa and Schuster (1988), more than 50 failed by overtopping as the result of an erosive breach by the overtopping water. Water quickly accumulated behind the Hsiaolin landslide dam as a consequence of upstream inflows due to the incessant rainfall. The tragic failure of the dam took place in minutes burying the entire Hsiaolin Village without any forewarning or enough time for emergency response.

The formation and failure of landslide dams are complex processes that occur at the interface between hillslopes and alluvial plain or valley-floor systems on the Earth's surface. Understanding, simulating, and predicting the occurrence, longevity, breakdown, and subsequent debris flows of landslide dams has attracted attention in many multidiscipline studies (Costa and Schuster, 1988; Li et al., 2002; Chen

* Corresponding author. Tel./fax: +886 3 4222964.
E-mail address: mli@cc.ncu.edu.tw (M.-H. Li).

0013-7952/$ – see front matter © 2011 Elsevier B.V. All rights reserved.
doi:10.1016/j.enggeo.2011.05.002

Table 1
The historical records of daily rainfalls greater than 400 mm/day observed at the Mintzu station and the corresponding daily averaged runoffs and runoff ratios at the Shanlin Bridge station.

Date	Daily Rainfall[a] (mm/day)	Daily Runoff[b] (m^3/s)	Runoff Ratio[a]	Typhoon Events
2 Jun 1977	445.3	–	–	–
25 Jul 1977	465.0	–	–	THELMA
29–30 Jul 1982	466.5	–	–	ANDY
	402.8	–	–	
13 Aug 1988	427.2	612.0	0.238	–
1 Aug 1996	484.0	2350.0	0.808	HERB
30 Jul 2001	466.0	1510.0	0.539	TORAJI
2–4 Jul 2004	530.0	615.8	0.193	MINDULLE
	451.0	1496.7	0.552	
	536.0	1633.2	0.507	
19 Jul 2005	626.0	1150.7	0.306	HAITANG
1 Sep 2005	621.0	980.3	0.263	TALIM
9 Jun 2006	473.0	913.7	0.321	–
19 Aug 2007	457.0	–	–	SEPAT
14 Sep 2008	438.0	–	–	SINLAKU
8 Aug 2009	1,114.0	1191.2	0.178	MORAKOT

[a] Runoff ratio was calculated as runoff depth divided by rainfall depth. Runoff depth is calculated as the runoff discharge divided by drainage area. "—" means data not available or not a typhoon event.

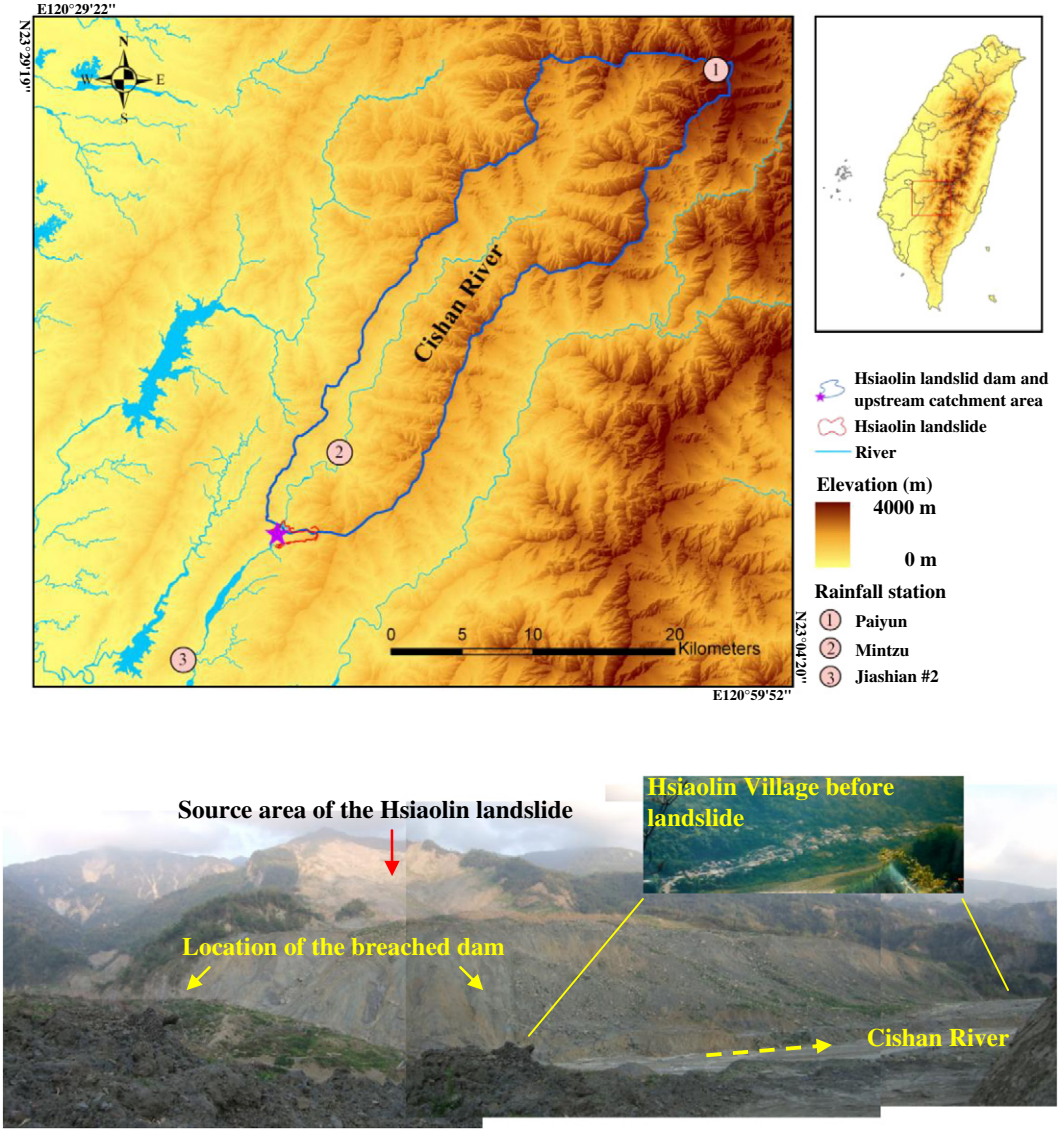

Fig. 1. The Hsiaolin landslide, the landslide dam and the buried Hsiaolin village. The landslide blocked the Cishan River and the landslide dam breached soon after the formation of an impounded lake. Blue line shows the drainage basin upstream of the Hsiaolin short-lived landslide dam. The boundary of the upstream catchment area is generated by the ArcHYDRO tool. The photo taken from the west bank of the Cishan River shows the breached dam.

et al., 2004; Korup, 2004; Iovine et al., 2007; Corominas and Moya, 2008; Crosta and Clague, 2009; Dong et al., 2009; Nandi and Shakoor, 2009; Dong et al., 2011). The longevity of landslide dams depends on many factors, such as rate of inflow into the impoundment, the size and shape of the dam, and its geotechnical characteristics. Based on 63 cases mentioned in the literature, 22% of landslide dams failed less than 1 day after formation (Schuster and Costa, 1986). Most, that is 85% of 73 recorded landslide dams failed within one year of formation (Costa and Schuster, 1988).

Seismic waves induced by massive landslides, observed by the Taiwan Central Weather Bureau Seismic Network, pinpointed the occurrence of the landslide at 06:16 (local time, UTC + 8) on 9 August (Tsou et al., 2011). Based on vivid descriptions of several eyewitnesses, the Cishan River had become completely dry right after a sudden loud rumbling bang, indicating the formation of the landslide dam. Within less than an hour, this short-lived dam collapsed and the massive debris flow buried the entire village. The locations of the Hsiaolin landslide, breached landslide dam, and the buried Hsiaolin Village can be found in Fig. 1 (as the Fig. 1 presented in Part I of this study with a focus on post-event reconstruction of the dam's geometry by Dong et al., in press).

Once a landslide dam has formed, water impoundment follows and sooner or later a landslide lake appears. Regardless of how long these types of lakes last, the reality is that residents living in downstream valleys are in great danger if and when overtopping or breaching of the dam occurs. Therefore in addition to spotting potential landslide sites, understanding the breaching process and the possible distribution of debris deposition is crucial to effective hazard mitigation and timely emergency response. In this part of study, the breaching process of the Hsiaolin landslide dam and the spatial and temporal characteristics of subsequent debris flow deposition were investigated numerically. To reasonably facilitate the simulation of mud flows induced by the landslide dam breach, the US National Weather Service BREACH model (Fread, 1991) was applied to generate the landslide dam break hydrograph which is then used as input to drive the Federal Emergency Management Agency approved FLO-2D model (O'Brien et al., 1993; O'Brien, 2006). A systematic integrated numerical approach was proposed and validated with data from the Hsiaolin tragedy. There is an urgent need to perform such numerical investigations for all susceptible landslide areas to help predict future landslide breach potentials and debris deposition distribution and for the planning of hazard mitigation measures.

2. Study area and hydrological analysis

2.1. Study area

Hsiaolin Village is located in southern Taiwan along the river terrace of the Cishan River, one of the major tributaries of the Gaoping River, having a drainage area of 842 km^2 and a main stream length of 118 km. The river is oriented northeast to southwest. For validation purposes during runoff simulation, we focus on the presentation of the Shanlin Bridge subbasin as shown in Fig. 2a. The drainage area of the Shanlin Bridge streamflow station is 519.5 km^2. The elevation varies from 115 m to about 3936 m, the slope range from 0° to 74.9° with a mean slope of 27.5°, based on analysis of 40 m resolution DTM data generated in 1989. The major land cover is evergreen forest, mixed hardwood forest, and river valleys.

2.2. Hydrological analysis

The study area has a tropical monsoon climate with rainfall being mainly contributed by typhoons and summer monsoons. The wet season (May to October) normally accounts for 90% of the annual rainfall in southern Taiwan (Li et al., 2009). The mean annual rainfall for the Cishan River area is about 3077 mm/year (HPEI, 2009). There

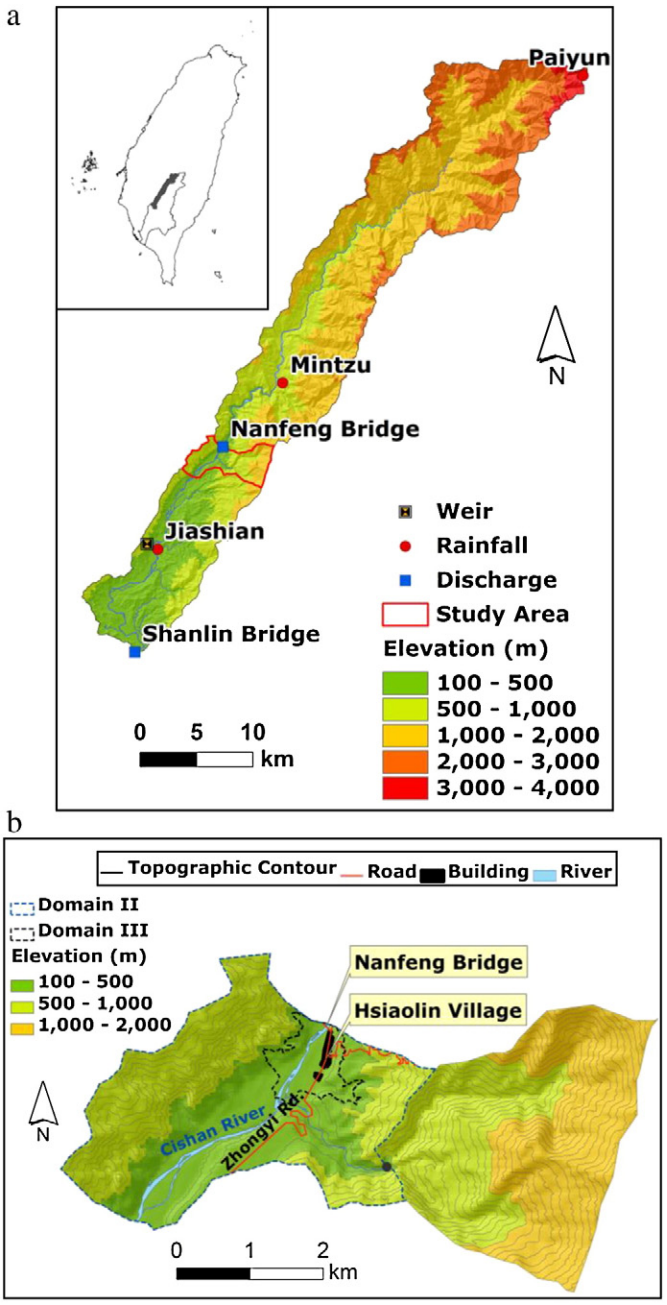

Fig. 2. (a) The Cishan River basin above the Shanlin Bridge station for Domain I simulation. (b) Vicinity of the Hsiaolin Village with topographic contours (50 m interval). Dashed blue and dashed black lines indicate the boundaries of Domain II and Domain III, respectively. Black dot indicates the outlet of the right subbasin detached to obtain the right boundary of Domain II.

are three rainfall stations (Jiashian 2, Mintzu, and Paiyun) and one streamflow station (Shanlin Bridge) in the study area (Fig. 2a). The Nanfeng Bridge streamflow station failed at 01:00 on 9 August. Rainfall gauge data are interpreted using the Thiessen Polygons method (Thiessen, 1911) to obtain basin-averaged rainfalls. The weighting factors determined for the rain stations of Jiashian 2, Mintzu, and Paiyun are 0.241, 0.416, and 0.343, respectively. The total basin-averaged rainfall during Typhoon Morakot was 1940 mm, accumulated from 14:00 of August 6 to 23:00 of August 10, in the Cishan River basin. The maximum hourly basin-averaged rainfall intensity of 70.7 mm/h was observed from 20:00 to 21:00 local time on 8 August 2009. Within three days, this typhoon event dropped more than 60% of the annual rainfall on this mountainous river basin.

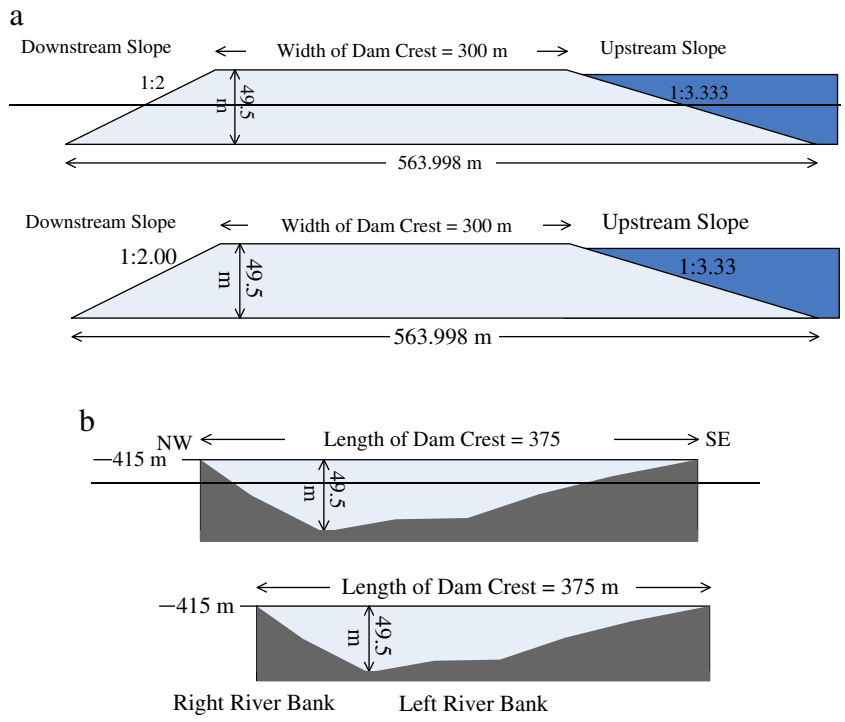

Fig. 3. Schematic diagrams of geometric characteristics of the Hsiaolin landslide dam for case of the dam crest elevation at 415 m. (a) Longitudinal dam profile along the Cishan River. (b) Cross sectional profile of the Cishan River valley near the Hsiaolin Village.

3. Methodology

The US National Weather Service BREACH model (Fread, 1991) was used to simulate the discharge hydrograph emanating from the breached Hsiaolin landslide dam with upstream inflows simulated by the Federal Emergency Management Agency approved FLO-2D model (O'Brien et al., 1993; O'Brien, 2006). The breached discharge hydrograph was then fed back to the FLO-2D model for debris deposition simulations.

3.1. Dam break routing and overland flood routing

The BREACH model is a physically based mathematical model capable of predicting the breach characteristics (e.g., size, shape, and time of formation) and the discharge hydrograph emanating from a breached earthen dam. The model was developed by coupling the conservation of mass for the reservoir inflow, spillway outflow, and breach outflow with the sediment transport capacity of the unsteady uniform flow along an erosion-formed breached channel. The bottom slope of the breach is assumed to be essentially that of the downstream face of the dam. The growth of the breach channel is dependent on the dam's material properties (e.g., D_{50} size, unit weight, friction angle, cohesive strength), which can be either homogenous or with the properties of the core material being different from those of the outer portions of the dam. Two types of dam failure scenarios, overtopping failure and piping breach, can be simulated by the model. For the short-lived Hsiaolin landslide dam, overtopping failure was mainly considered in this study as discussed in Section 7.3 of the Part I paper (Dong et al., in press). Input data requirements include the dam's geometry, the texture of the material, the relationship between the water level and the surface area of the landslide dam lake, the time-dependent reservoir inflow rate to a landslide dam lake, and the spillway characteristics. For more detail descriptions of the model can be found in Fred (1991).

The FLO-2D model is a physically based, distributed flood-routing model using the fully dynamic wave momentum equation and a central finite-difference routing scheme. For rainfall-runoff simulations, the FLO-2D provides river routing and surface runoff modules taking into account the forcing of the rainfall and/or inflow hydrograph. River flow is described as a one-dimensional multiple channel network. Surface runoff is interpreted as a two-dimensional overland flow regime. The interactions between river flow and surface runoff can occur with overland return flow to the channel or as overbank discharge when the flow exceeds the channel capacity. Infiltration and evapotranspiration processes are optional modules.

The FLO-2D model also provides modules to simulate two-dimensional sediment transport, hyperconcentrated debris and mud flow. The total shear stress in hyperconcentrated sediment flows, including debris flows, mudflows and mud floods, is calculated from

Table 2
Estimated geometric characteristics of Siaolin landslide dam with a fixed bottom elevation of 365.5 m.

Crest elevation of dam (m)	430	425	420	415	410
Height of dam (m)	64.5	59.5	54.5	49.5	44.5
Crest width of dam (m)	300	300	300	300	300
Crest length of dam (m)	465	415	400	375	340
Equivalent length of dam crest (m)	245.2	225.0	213.4	208.3	192.1
Volume of dam (m^3)	7,464,851	6,140,387	5,179,350	4,454,279	3,365,233
Landslide lake capacity (m^3)	25,252,344	20,548,300	15,286,983	12,431,518	9,776,734
Time required for landslide lake to reach overtopping (h)	>2.03	1.65	1.28	0.97	0.73

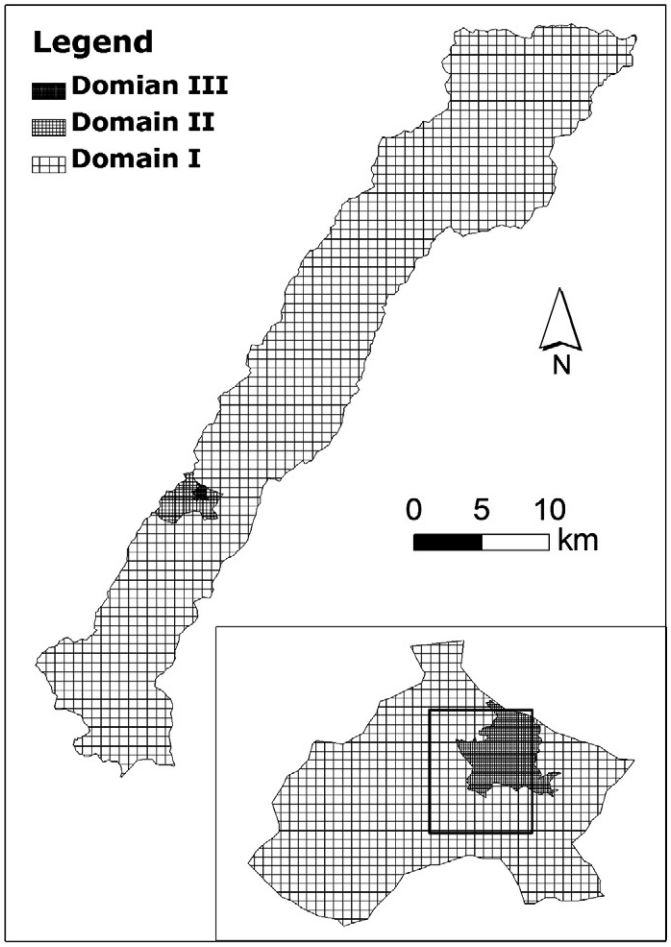

Fig. 4. Simulation domain setting (Hierarchical Framework) of FLO-2D includes coarse (Domain I, 200 m), median (Domain II, 40 m), and fine (Domain III, 10 m) for rainfall-runoff simulation, and mudflow simulation focus around Hsiaolin Village, respectively. Lower right corner is the simulation domain setting around the Hsiaolin Village.

the summation of the cohesive yield stress, the Mohr-Coulomb shear stress, the viscous shear stress, the turbulent shear stress, and the dispersive shear stress. The quadratic rheological model is employed in the FLO-2D model to describe the processes of the debris flow/mudflow. The quadratic rheological model utilizes empirical equations of an exponential type and requires 2 pairs of empirical coefficients (α and β) for yield stress and viscosity to be described as functions of the sediment concentrations (O'Brien, 1986). In most cases, the volumetric sediment concentration of such a fluid matrix ranges from roughly 30–55% depending on the relative proportion of silts and clays (sediments).

The total friction slope (S_f) of hyperconcentrated sediment flows in the momentum equation is described as (O'Brien, 2006),

$$S_f = S_y + S_v + S_{td} = \frac{\tau_y}{\gamma_m h} + \frac{K\ \eta\ V}{8\gamma_m\ h^2} + \frac{n_{td}^2 V^2}{h^{4/3}} \quad (1)$$

where S_y is the yield slope; S_v is the viscous slope; S_{td} is the turbulence dispersive slope; h is the hyperconcentrated sediment depth; V is the depth-averaged velocity; $\tau_y$is the yield stress parameterized as $\tau_y = \alpha_2 \cdot \exp(\beta_2 \cdot C_V)$; $\gamma_m$is the specific weight of the sediment mixture; K is the resistance parameter; η is the viscosity of the sediment mixture parameterized as $\eta = \alpha_1 \cdot \exp(\beta_1 \cdot C_V)$; $n_{td}$is the turbulent flow resistance n-value parameterized as $n_{td} = 0.0538 \cdot n \cdot \exp(6.0896 \cdot C_V)$; α_1, α_2, β_1, and $\beta_2$are empirical coefficients as defined by laboratory experiments (O'Brien and Julien, 1988); C_v is sediment concentration by volume. More details of the model description and numerical algorithms can be found in O'Brien (2006).

3.2. Geometric characteristics of the Hsiaolin landslide Dam for Dam break routing

The Hsiaolin landslide dam was a short-lived earthen dam. About an hour after its formation, the landslide dam had failed due to overtopping. The exact geometric characteristics (e.g., crest elevation, side slopes, dam volume, etc.) of the dam can only be reconstructed by post-event investigation based on available pieces of field evidence and the hydrological constraints as presented in the Part I study. The estimated landslide area and volume are 620,000 m^2 and 2520×10^4 m^3, respectively. About 64% (1530×10^4 m^3) of the earth materials slid downhill

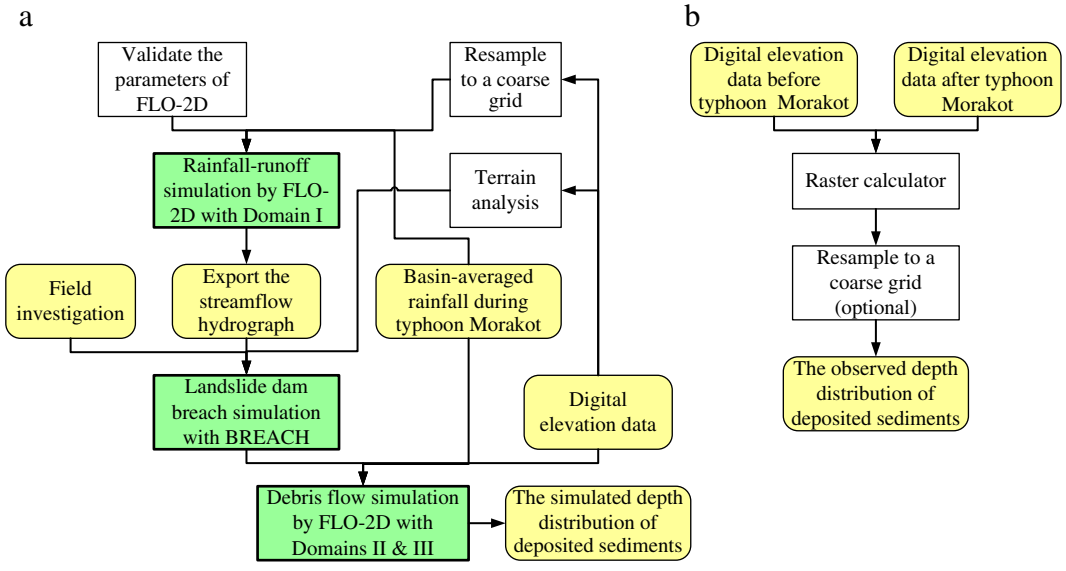

Fig. 5. Flowcharts of (a) the integrated models approach and (b) DTMs processing to obtain depths of sediment depositions. The rounded rectangles, rectangles with thin line, and rectangles with solid line are the input/output data, data processing, and model simulations, respectively.

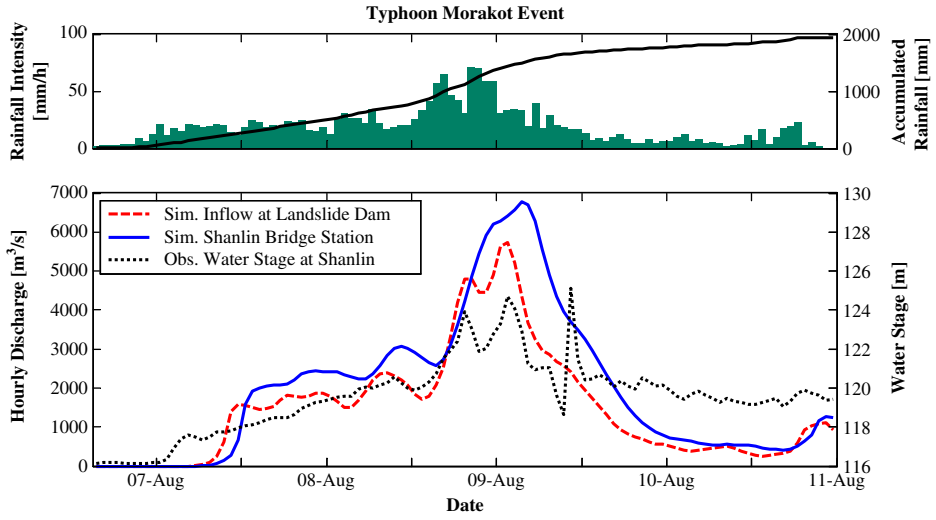

Fig. 6. The results of rainfall-runoff simulation during typhoon Morakot (from 14:00 of August 6 to 23:00 of August 10). (Top) The basin-averaged rainfall histogram, and the thick solid line represents the accumulated rainfall. (Bottom) Simulated hydrographs at the Shanlin Bridge (dashed red line) and at the upstream side of the landslide dam (solid blue line), and the observed water stages at the Shanlin Station (dashed black line).

into the bed of the Cishan River near the upstream side of the Nanfeng Bridge (Dong et al., in press).

According to the post-disaster field investigations conducted by Lee et al. (2009), they concluded that the landslide dam was a frustum-shape type. Without hard evidence for dam crest elevations, five different dam geometric characteristics were conceptualized for changing crest elevations, ranging from 410 to 430 m at intervals of 5 m, with fixed gradients on the downstream and upstream sides (i.e., 2.00 and 3.33, respectively, as shown in Fig. 3a) while performing BREACH simulations in this part of the study. Table 2 lists the geometric characteristics for five different cases, including dam crest width, dam crest length, equivalent length of dam crest calculated for the given dam crest elevation and the valley topography. The transverse profile of the Cishan River valley near the Hsiaoling village has an asymmetric pattern. The right river bank (i.e., the right-hand side of a river when facing downstream) has a steeper gradient than the left river bank as shown in Fig. 3b.

3.3. Integrated simulation approaches

To simulate rainfall-runoffs and debris flows of the entire Cishan River basin with high spatial resolutions is not practical when the point of interest is the vicinity of Hsiaolin Village. The hydrologic constraints required for model validation are the observed streamflow data from gauge stations. Three nested simulation domains, as shown in Fig. 4, were prepared for FLO-2D simulations. A total of 3 DTM data was used in this study. The 40 m DTM was generated before the Typhoon Morakot. Two 5 m resolution DTMs were available before and after the event, but only for a small area covering the vicinity of Hsiaolin Village. Domain I is the drainage basin of the Shanlin Bridge station as shown in Fig. 2a and Fig. 4 for grids. The Nanfeng Bridge station is located about 30 km upstream of the Shanlin Bridge station. The spatial resolution of Domain I grids is 200 m upscaled from the 40 m DTM and the total grid number is 12,202 as used for validation purposes and to provide inflow hydrographs for BREACH simulations.

Domain II is the vicinity of Hsiaolin Village, covering a subbasin from the Nanfeng Bridge station to about 2 km downstream of the Nanfeng Bridge station (see dashed blue line in Fig. 2b for Domain II boundary and Fig. 4 for grids). The right boundary of Domain II was determined by detaching a subbasin using the outlet at an elevation of 478 m as the black dot shown in Fig. 2b. The left boundary of Domain II is the natural watershed divide. The spatial resolution of Domain II grids is 40 m and the total grid number is 6296 as used for integration with the BREACH dam break outflow hydrographs.

Domain III covers a subbasin from the Nanfeng Bridge station to about 1.2 km downstream of the Nanfeng Bridge station (see dashed black line in Fig. 2b for Domain II boundary and Fig. 4 for grids). The left and right boundaries of Domain III were taken at an elevation of 450 m. Domain III is the finest domain with a spatial resolution of 10 m and a total grid number of 9032. It is noted that Domain III grids were constructed by upscaling the 5 m DTM before the Typhoon

Table 3
Model parameters used for FLO-2D simulations in this study.

Parameters	Units	Value	Source
α_1 for Viscosity	[0.1 Pa·s]	0.00462	Lin et al.(2005)
β_1 for Viscosity	[−]	11.24	Lin et al.(2005)
α_2 for Yield stress	[0.1 Pa]	0.811	Lin et al.(2005)
β_2 for Yield stress	[−]	13.72	Lin et al.(2005)
K (resistance parameter)	[−]	2285	O'Brien (2006)
Specific gravity of sediment, G_s	[−]	2.70	Lin et al.(2005)
Manning's roughness coefficient, n, for river	[−]	0.045	Calibration
Manning's roughness coefficient, n, for surface	[−]	0.600	Calibration

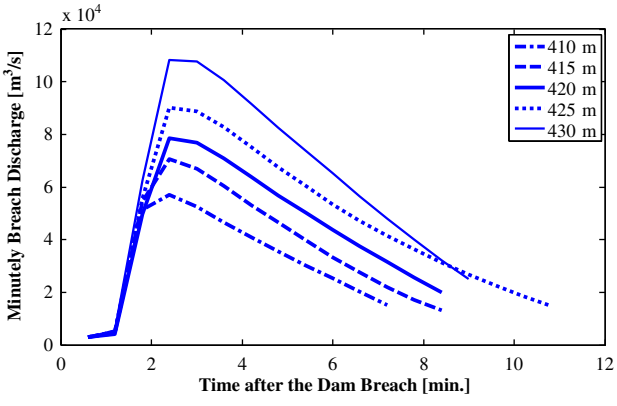

Fig. 7. Dam breach hydrographs simulated by BREACH with different dam crest elevations.

Table 4
The characteristics of dam breach hydrographs simulated by BREACH.

Crest elevation of dam [m]	430	425	420	415	410
Duration of dame breach [min]	9.0	10.8	8.4	8.4	7.2
Peak discharge [cms] (the time after the dam breach [min])	108,242 (1.8)	90,036 (1.8)	78,591 (1.8)	70,649 (1.8)	56,905 (1.8)
Original sedimentation concentration by volume	0.230	0.208	0.235	0.241	0.244
1.5 times the original sedimentation concentration by volume	0.345	0.312	0.353	0.362	0.367

Morakot. Simulation results of Domain III were used for comparison with the post-event debris deposition depth estimated by the differences of DTMs before and after the event.

In this study, a series of integrated simulations was conducted as depicted in the flowchart in Fig. 5a. Our approach mainly contains three steps:

(1) The Domain I grids were used for the first step in the simulations. The rainfall-runoff was simulated by FLO-2D from 14:00 local time on 6 August to 23:00 on 10 August. Top of Fig. 6 shows the hourly basin-average rainfall data calculated with the Thiessen polygons approach from rainfall amounts observed at 3 rain gauge stations (Fig. 2a). The Manning's roughness coefficients for rivers and surfaces (bottom of Table 3) were calibrated from hourly streamflow data observed at the Shanlin Bridge station during Typhoon Herb (1996). It is noted that the runoff ratio (Table 1) computed at the Shanlin Bridge Station during Typhoon Morakot is too small to be used for validation. The purpose of this simulation step is to provide inflow hydrographs for BREACH simulations.

(2) The BREACH model was employed for the second step of the simulation, for the different crest elevation scenarios listed in Table 2, to obtain dam break outflow hydrographs to be used for the Domain II and III simulations. The Hsiaolin landslide dam was assumed to have occurred at 06: 16 on 9 August, the same time that the massive landslide occurred, as presented in Part I of this study. The spatial distributions of the deposited sediments was calculated with DTMs before and after Typhoon Morakot, as in the flow chart depicted in Fig. 5b. This will be compared with the spatial distribution of sediment depths computed in the third step of the simulations.

(3) In the third step of the simulations mudflow routings obtained using the FLO-2D model for Domains II and III, from 06:00 to 08:00 local time on 9 August, were combined with the input of dam break hydrographs computed by the BREACH model. The average sediment concentration by volume was first estimated as the ratio of landslide dam volume to the total volume of dam break hydrograph, and then adjusted as values suggested in O'Brien (2006).

4. Results and discussions

4.1. Rainfall-runoff simulations with domain I grids

The top of Fig. 6 shows the basin-average rainfall histogram used to drive FLO-2D simulations with Domain I grids and the accumulated rainfall (thick solid line). It is noted that the sharpest rainfall accumulation appeared in the early morning of 9 August, just prior to the occurrence of the massive landslide at 6:16. The bottom of Fig. 6 shows the simulated hydrographs at the Shanlin Bridge (dashed red line) and for the upstream side of the landslide dam (solid blue line), as well as the observed water stages at the Shanlin Station (dashed black line). Obviously the third peak of observed stages was the evidence of upstream dam breaching as there were only two rainfall peaks. Since the Domain I simulations were performed without dam breaching, only two peaks appeared in the simulated discharges at the upstream side of the landslide dam (solid blue line in the bottom of Fig. 6). The peak discharge rates at the Shanlin Bridge and upstream of the landslide dam were 6786 m^3/s at 03:00 and 5727 m^3/s at 01:00, respectively, on 9 August (Fig. 6). The reason that we did not use the observed discharges at the Shanlin Station for calibration is the computed runoff ratio (i.e., runoff-depth/rainfall-depth) during Typhoon Morakot was only 0.178 (Table 1). This is not consistent with normal runoff ratios during extreme events in Taiwan. For three typhoons examined by Li et al. (2005), the runoff ratios for typical mountainous watersheds in Taiwan were from 0.58 to 0.7. Domain I grids with FLO-2D were first calibrated by Typhoon Herb (1996) to determine Manning's roughness coefficients (see bottom of Table 3), and the simulated discharges at the upstream side of the landslide dam (solid blue line in the bottom of Fig. 6) were then used as the inflow constraints for BREACH simulations. As presented in the Part I study, the estimated landslide dam formation time was 06:16 on 9 August. An average inflow discharge of 2974 m^3/s (between 06:00 and 07:00 local time on 9 August (Fig. 6) was used as the inflow rate

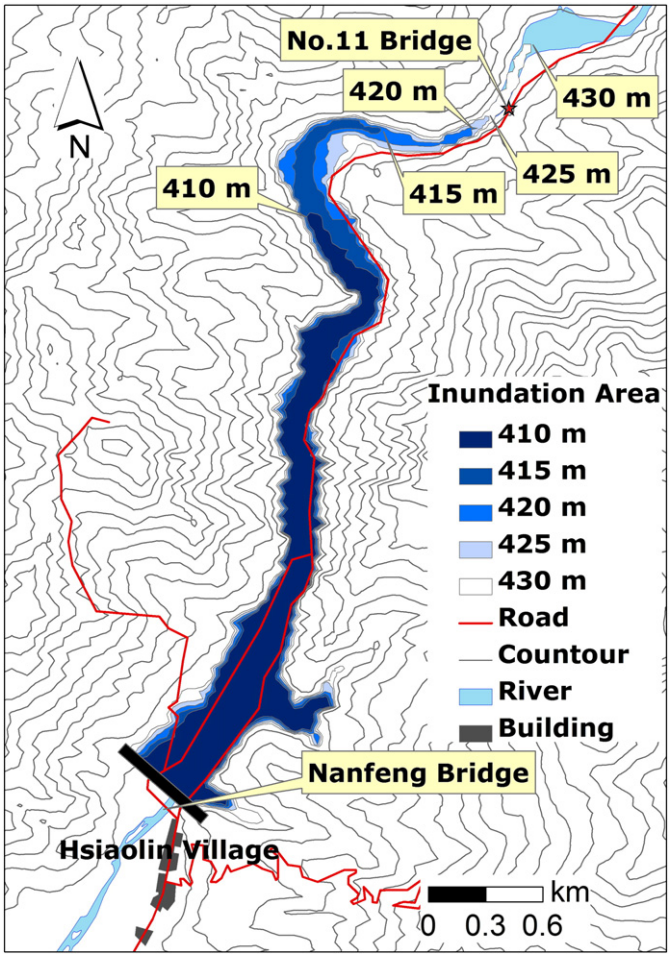

Fig. 8. Inundation areas of the landslide lakes estimated with different dam crest elevations and same inflow rates determined by FLO-2D simulations with Domain I grids.

for calculating the time required for the landslide lake to reach the depth for overtopping to occur.

4.2. Landslide Dam breach simulations

For short-lived landslide dams, the most critical and difficult issue involved in using the BREACH for dam break simulation is estimation of the dam crest elevation. Numerical experiments were conducted to determine the most likely crest elevation given several hydrological and hydraulic constraints. Five different dam possible crest elevations varying from 410 m to 430 m at intervals of 5 m were simulated by the BREACH with the corresponding dam geometric characteristics listed in Table 2. The major differences among the different dam crest elevations used in this study are the volume of the earthen dam, the capacity of the landslide lake, and the time required to reach overtopping. In the case with a higher dam crest elevation, the volume of the dam and reservoir capacity would be larger, and a longer time would be required to reach the point of overtopping than when the elevation of the crest is lower. It should be noted that variations in the dam volume and landslide lake capacity are not linearly related to the crest elevation due to the mountain valley topography.

Fig. 7 depicts the dam breach hydrographs computed by the BREACH with different dam crest elevations. Since the dam was short-lived, the dam breach hydrographs were presented as the minutely average discharges. As can be seen, the crest elevation is a critical factor affecting the peak discharge amount and the time of the breach outflow hydrographs. Other characteristics of the breach hydrographs computed by BREACH are listed in Table 4. The sediment concentration by volume (required for FLO-2D simulations) was originally estimated as the ratio of earthen dam volume to total volume of earthen dam and landslide lake water. The variances in sediment concentration by volume were from 0.208 (dam crest elevation at 425 m) to 0.244 (dam crest elevation at 410 m). It should be noted that the major difference in computed breach outflow hydrographs for the different crest elevations is the peak discharge amount (Table 4 and Fig. 7).

The first constraint that can be applied to determine the most likely crest elevation is the time required for the landslide lake to reach overtopping. This varied with the crest elevation. The capacities of landslide lakes for different dam crest elevations were 25.3, 20.5, 15.3, 12.4, and 9.8 million m^3 (see Table 2). The shortest time was only 0.73 h when the crest elevation was 410 m. The longest time was more than 2 h for a crest elevation of 430 m. The time required for overtopping was then used to determine the time that FLO-2D simulated discharges in the Domain I grid to be used as the upstream inflows after the cease of dam break hydrograph. Based on eyewitness descriptions, the landslide dam failed within 1 h of formation, suggesting the dam crest elevations to be less than 420 m (see Table 2).

The second constraint is the inundation area/boundary of the landslide lake. Based on different crest elevations, DTMs, and spatial surface water depths before dam breach and upstream inflow rates computed by FLO-2D with Domain I grids, the upstream backwater limitations of different crest elevations were determined as delineated in Fig. 8. The backwater limitation might vary from 3.7 km (for a dam crest elevation of 410 m) to 5.6 km (for dam crest elevation of 430 m) away from the Nanfeng Bridge (Fig. 8). As presented in Section 5 of the part I study, the landslide backwater may reach as far as the No. 11 Bridge (Fig. 8) indicating the presumed dam crest elevation should be at least 410 m. Based on the first two constraints, the dam crest elevation was most likely between 410 m and 420 m.

The third constraint is the spatial distribution of sediment deposition as determined from the DTMs before and after Typhoon Morakot. Mudflow simulations were conducted for all 5 cases using the FLO-2D with the Domain II grid. The simulation results will be discussed in the next subsection.

4.3. Mudflow simulations with domain II grids

The depth of sediment depositions was estimated from differences in the DTMs before and after Typhoon Morakot (2009), as shown in Fig. 9. As depicted in Fig. 5b, the original sediment depth distribution with a 5 m resolution (Fig. 9a) was upscaled to a 40 m resolution (Fig. 9b) for calibrating the simulation results with the Domain II grids. The spatial distributions of dam break debris were confined within the Cishan River valley due to the steep mountainous topography. The village of Hsiaolin was located on a terrace on the left-hand bank of the Cishan River, right in the path the massive mudflows induced by the landslide dam breach. There were numerous casualties because there was no timely landslide warning issued.

The computed dam breach hydrographs (Fig. 7) were combined with the computed streamflow discharges (Fig. 6) from Domain I grids to drive mudflow simulations by FLO-2D with Domain II grids

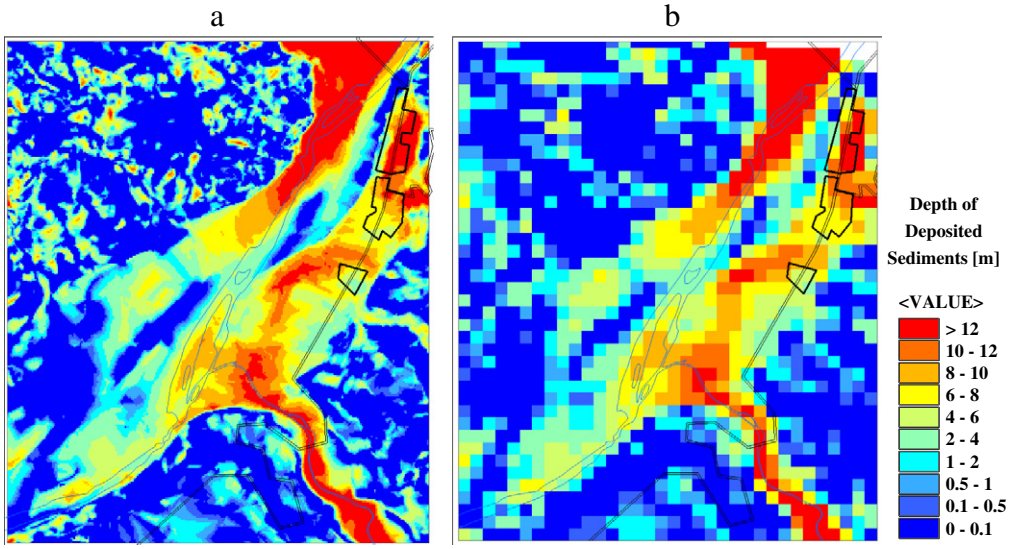

Fig. 9. Depths of sediment depositions estimated by differences of DTMs before and after Typhoon Morakot (2009) (a) with fine resolution (5 m), and (b) with coarse resolution (40 m, spatial average of fine grid). Bold line polygons represent the building blocks (Hsiaolin Village), parallel line represents the roads, and thin line represents the river bed of Cishan River.

using the original sediment concentration by volume (Table 4). Table 3 listed parameters used for the FLO-2D mudflow simulation. Since there is no experimental data available for field materials, values were adopted from Lin et al. (2005) for performing simulations. Observed and computed sediment depths distributions around the Hsiaolin Villages were compared in Fig. 10. Based on the observed

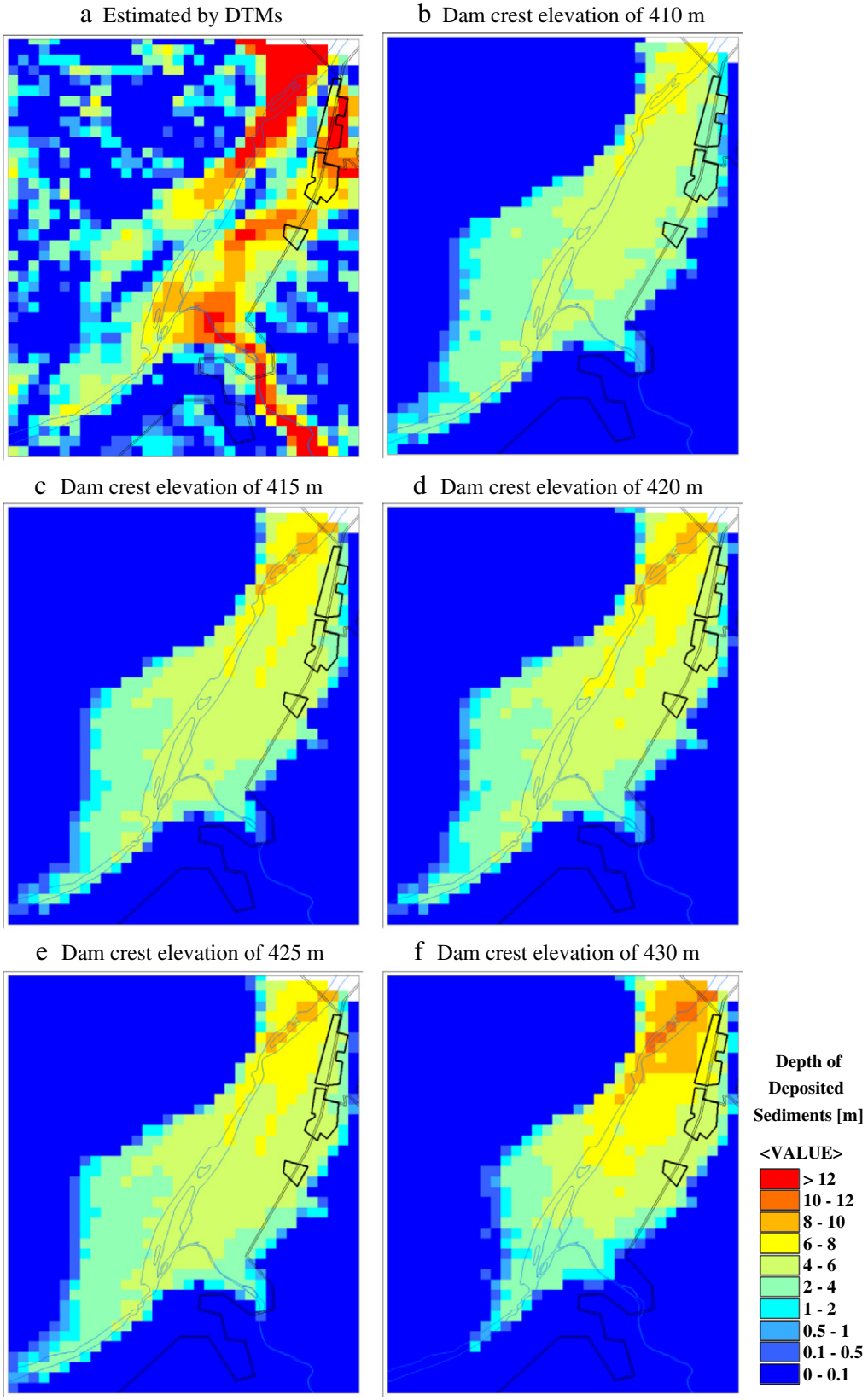

Fig. 10. Depths of sediment depositions around the Hsiaolin Village simulated by FLO-2D with dam break outflow hydrographs computed by BREACH with different dam crest elevations using the original sediment concentration by volume as listed in Table 4. The spatial resolution is 40 m.

depths estimated by DTMs differences (Fig. 10a), there was a slight detour in the main river course to the left. Zero depths (dark blue) on the right bank of the original channel indicate significant scouring and deposition after the dam broke. Such mixed scouring and deposition is beyond the limitations of the current model. The spatial distribution patterns were similar for all 5 simulated cases. However,

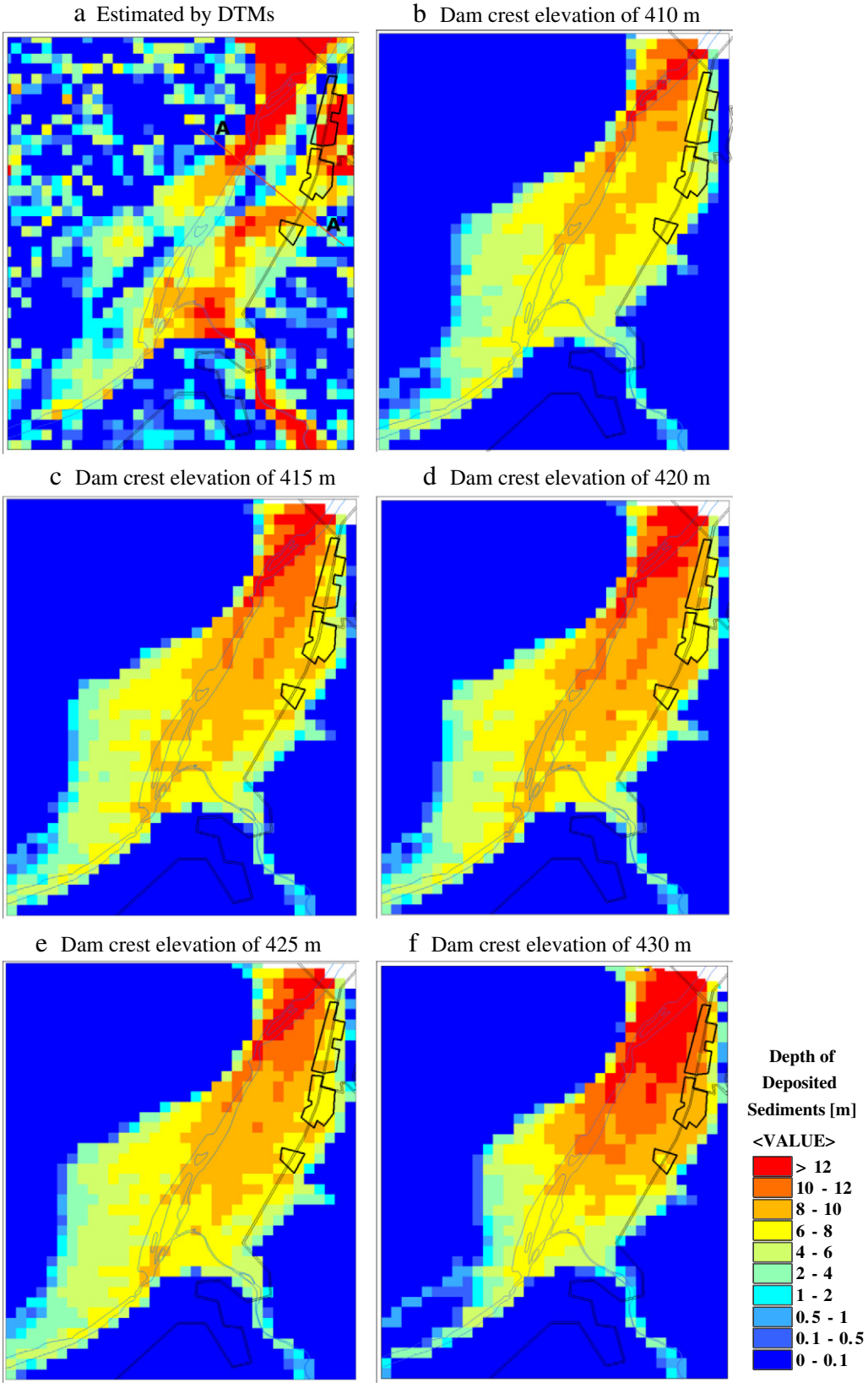

Fig. 11. Depths of sediment depositions around the Hsiaolin Village simulated by FLO-2D with dam break outflow hydrographs computed by BREACH with different dam crest elevations using 1.5 times of the original sediment concentration by volume as listed in Table 4. The spatial resolution is 40 m.

Table 5
The results of mudflow simulations with different dam crest elevations.

Dem crest elevation	Spreading distance along the river (m)	Freeze time (min)	Estimated mudflow velocity (m/s)	Spreading width along the line AA (m)	Average depth along the line AA (m)
410 m	1475	3:36	6.8	518	7.02
415 m	1503	3:36	7.0	518	8.03
420 m	1532	3:36	7.1	518	8.48
425 m	1560	3:36	7.2	518	7.97
430 m	1430	3:00	7.9	518	9.47
415 m (10 m resolution)	–	3:36	–	495.7	9.30
Observation	1500	–	–	523.8	–

Note: The transection line AA was shown in Fig. 12 of the Part I study.

the computed sediment depths were much lower than the observed values.

At first, it was suspected that the reason the computed sediment depths were less was underestimation of the stream flow discharge by FLO-2D. The time of forming and breaching of the Siaoline landslide dam appeared at the period of the recession limb of the stream flow hydrographs. It is possible that the stream flow after peak discharge could be underestimated because subsurface return flow was not considered in FLO-2D (Li et al., 2005). To see the effect of large upstream inflow on breach outflows, the discharge amount (Fig. 6) was multiplied 1.2 and 1.4 times and the BREACH rerun. The results (not shown herein) for larger upstream flows significantly reduced the time required to reach overtopping, but there was an insignificant increase in the breach outflow amounts.

The next attempt we focused on errors induced by underestimation of the sediment concentration by volume. As depicted in Fig. 15 of the Part I study, there are two dams generated after massive landslides, but only Dam A was considered in this study due to simplifications. To account for sediments contributed by Dam B, we artificially enlarge the sediment concentration by volume by 1.5 times for all 5 cases as shown in the bottom of Table 4, and reran FLO-2D mudflow simulations. Fig. 11 presents DTMs estimated and the FLO-2D computed sediment depths distributions around the Hsiaolin Village. For crest elevations of 415 m, 420 m, and 425 m, the overall pattern of deposited sediment, in terms of spatial distribution and depth, can be well simulated by the model, with the simulated depths reaching as high as 12 m.

Table 5 listed mudflow characteristics retrieved from FLO-2D results. Differences among 5 cases simulated were not significant; however there are not enough field observations available for validations. Dam break mudflow may reach 1.5 km downstream of the landslide dam which is close to that retrieved from DTMs. Also the spreading widths along the transection line AA (see Fig. 13 in the Part I study) computed by FLO-2D are also close to that retrieved from DTMs. The third constraints of spatial sediment distributions concluded that the original sediment concentration by volume was underestimated, and 1.5 times of the original values with crest elevations from 415 m to 425 m captured the debris distribution well. According to O'Brien (2006), the sediment concentration by volume should be 0.35–0.40 to have marked setting of gravels and cobbles in mud flood events.

Based on the above discussions, the following conclusions can be drawn. The first constraint suggested that the crest elevation should be less than 420 m. The second constraint recommended that the crest elevation should be between 410 m and 415 m. The third constraint proposed that the crest elevations should be between 415 m and 425 m and the sediment concentration by volume should be 1.5 times the original estimates. A crest elevation of 415 m and a sediment concentration by volume of 0.362 (Table 4) were used for FLO-2D mudflow simulations with Domain III grids.

4.4. Mudflow simulations with domain III grids

Fig. 12 presents the DTMs estimated and FLO-2D computed sediment depths distributions around the Hsiaolin Villages with a 10 m resolution. The overall sediment distribution pattern and depths can be well captured by this finer spatial resolution grid than those by the Domain II grid (Fig. 11c). It should be noted that some sediment depositions that appeared on the building blocks as shown in Fig. 12a were not captured in the mudflow simulations. Since the buildings were located on a river terrace, at least 10 m higher than the river bed, the sediment deposition was likely caused by a direct landslide rather than the dam breakage. However, this is only a speculation. There is no hard scientific evidence at current stage.

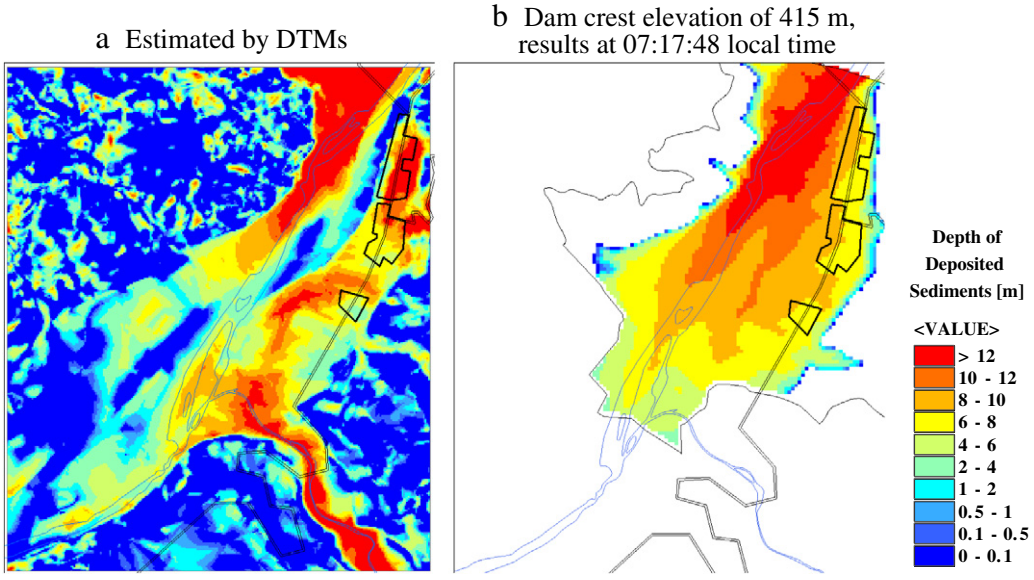

Fig. 12. Depths of sediment depositions around the Hsiaolin Village simulated by FLO-2D with dam break outflow hydrographs computed by BREACH with the dam crest elevation of 415. The spatial resolution is 10 m.

Some sediment depositions that appeared on the bottom right-hand corner in Fig. 12a were not simulated with the Domain II grids (Fig. 11) and outside of Domain III grids. More than 10 m of sediment deposition appeared along the tributary. It was concluded from the field investigation (Lee et al., 2009) that the sediment deposition was contributed by local landslides upstream of that creek, and was unrelated to the major landslide dam breach. Therefore simulations of those sediment depositions were not included herein. It is noted that some near zero depositions appeared in Figs. 11a and 12a, which indicated that some sediments were scoured away after landslide dam breach. The upstream continuing inflows may have washed way the dam break debris and detour the main channel.

5. Conclusions

An integrated simulation approach combining the BREACH and FLO-2D models was conducted to investigate the causes of the Hsiaolin tragedy during Typhoon Morakot (2009). Based on several hydrological and hydraulic constraints, it is suggested that the most likely crest elevation of the five simulated cases analyzed in this study was 415 m. Based on this elevation, the time required for the landslide lake to reach the point of overtopping would be 0.97 h, which would place the initiation of breaching around 07:14 (the landslide dam formed at 06:16 on 9 August). It only took about 8 min to reach complete breaching. However several factors might significantly affect these findings. For example, the conceptualized BREACH dam geometry might be quite different from reality. There is also a lack of accurately observed discharge data during this event for validation of the accuracy of FLO-2D model.

In view of hazard mitigation of landslide dams, understanding the breaching processes and the possible distribution of debris distributions is crucial to the planning of mitigation and response measures. The integrated modeling approach conducted herein can provide quantitative information with various temporal and spatial resolutions. However the success of such an integrated approach relies on model capabilities and a sufficiency of supporting material, including hydrological, geological, geomechanic, and geomorphic information.

Acknowledgments

This study was supported by the National Science Council of Taiwan through the National Central University under Grant NSC-98-2745-M-008-013. Valuable hydrometeorological data were provided by the Central Weather Bureau and Water Resources Agency in Taiwan. The authors are grateful for their support and thank constructive comments of the editor and anonymous reviewers to improve the original manuscripts greatly.

References

Chen, C.C., Chen, T.C., Yu, F.C., Hung, F.Y., 2004. A Landslide Dam Breach induced Debris Flow—A Case Study on Downstream Hazard Areas Delineation. Environmental Geology 47, 91–101.
Corominas, J., Moya, J., 2008. A review of assessing landslide frequency for hazard zoning purposes. Engineering Geology 102 (3–4), 193–213.
Costa, J.E., Schuster, R.L., 1988. The formation and failure of natural dams. Geological Society of American Bulletin 100, 1054–1068.
Crosta, G.B., Clague, J.J., 2009. Dating, triggering, modelling, and hazard assessment of large landslides. Geomorphology 103 (1), 1–4.
Dong, J.J., Tung, Y.H., Chen, C.C., Liao, J.J., Pan, Y.W., 2009. Discriminant analysis of the geomorphic characteristics and stability of landslide dams. Geomorphology 110, 162–171.
Dong, J.J., Tung, Y.H., Chen, C.C., Liao, J.J., Pan, Y.W., 2011. Logistic regression model for predicting the failure probability of a landslide dam. Engineering Geology 117, 52–61.
Dong, J.J., Li, Y.S., Kuo, C.Y., Sung, R.T., Li, M.H., Lee, C.T., Chen, C.C., Lee, W.R., in press. Forming and breaching of a short–lived landslide dam at Hsiaolin Village, Taiwan - Part I: Post-event reconstruction of dam geometry. Engineering Geology. doi:10.1016/j.enggeo.2011.04.001.
Fread, D.L., 1991. BREACH: an erosion model for earth dam failures. Hydrologic Research Laboratory, US National Weather Service.
Hydraulic Planning and Experimental Institute (HPEI), 2009. Strengthening water supply system adaptive capacity to climate change in Gaoping River basin. Water Resources Agency, Ministry of Economic Affairs, Taiwan. (in Chinese).
Iovine, G., Gregorio, S.D., Sheridan, M.F., Miyamoto, H., 2007. Modelling, computer-assisted simulations, and mapping of dangerous phenomena for hazard assessment. Environmental Modelling & Software 22 (10), 1389–1391.
Korup, O., 2004. Geomorphometric characteristics of New Zealand landslide dams. Engineering Geology 73, 13–35.
Lee, C.T., Dong, J.J., Lin, M.L., 2009. Geological investigation on the catastrophic landslide in Siaolin Village. Southern Taiwan. Sino-Geotechnics 122, 87–94 (in Chinese).
Li, M.H., Hsu, M.H., Hsieh, L.S., Teng, W.H., 2002. Inundation potentials analysis for Tsao-Ling landslide lake formed by Chi-Chi earthquake in Taiwan. Natural Hazards 25, 289–303.
Li, M.H., Yang, M.J., Soong, R.T., Huang, H.L., 2005. Simulating typhoon floods with gauge data and mesoscale modeled rainfall in a mountainous watershed. Journal of Hydrometeorology 6 (3), 306–323.
Li, M.H., Tien, W., Tung, C.P., 2009. Assessing the impact of climate change on the land hydrology in Taiwan. Paddy and Water Environment 7, 349–356.
Lin, M.L., Wang, K.L., Huang, J.J., 2005. Debris flow runoff simulation and verification – case study of Chen-You-Lan Watershed, Taiwan. Natural Hazards and Earth System Sciences 5, 439–445.
Nandi, A., Shakoor, A., 2009. A GIS-based landslide susceptibility evaluation using bivariate and multivariate statistical analyses. Engineering Geology 110, 11–20.
O'Brien, J.S., 2006. FLO-2D user's manual, version 2006. .
O'Brien, J.S., Julien, P.Y., 1988. Laboratory analysis of mudflow properties. Journal of Hydraulic Engineering 114 (8), 877–887.
O'Brien, J.S., Julien, P.Y., Fullerton, W.T., 1993. Two-dimensional water flood and mudflood simulation. Journal of Hydraulic Engineering 119 (2), 244–261.
O'Brien, J.S., 1986. Physical processes, rheology and modeling of mudflows. Doctoral dissertation, Colorado State University, Fort Collins, Colorado.
Schuster, R.L., Costa, J.E., 1986. A perspective on landslide dams. In: Schuster, R.L. (Ed.), Landslide Dam: Processes Risk and Mitigation. American Society of Civil Engineers, No. 3. Geotechnical Special Publication, pp. 1–20.
Thiessen, A.H., 1911. Precipitation for large areas. Monthly Weather Review 39, 1082–1084.
Tsou, C.Y., Feng, Z.Y., Chigira, M., 2011. Catastrophic landslide induced by Typhoon 912 Morakot, Shiaolin, Taiwan. Geomorphology 127, 166–178.